Probabilistic Earthquake and Flood Loss Assessment in the Middle East

Jamal Dabbeek, Vitor Silva, Carmine Galasso, Andrew Smith

Abstract

Investing in disaster risk reduction and resilience-increasing strategies requires a comprehensive understanding of multi-hazard risk. In this study, we assess the direct economic impacts of earthquakes, fluvial and pluvial floods on the residential building stock of 12 countries in the Middle-East: Jordan, Syria, Palestine, Saudi Arabia, Lebanon, United Arab Emirates, Yemen, Oman, Kuwait, Qatar, Bahrain and Iraq. The model provides the average annual losses as well as losses corresponding to various return periods available at the national and sub-national level. We estimate risk using a set of stochastic events considering a wide range of uncertainties. Specifically, the hazard component includes a regional probabilistic seismic hazard model considering uncertainty in the seismic sources/ruptures and ground motion models; and a high-resolution probabilistic flood hazard model for both fluvial and pluvial events. The loss model incorporates a high-resolution exposure database suitable for multi-hazard risk assessment. The vulnerability component considers diverse building typologies defined by material, lateral-load resisting system, building height, presence of basements and seismic design level. The findings are essential for raising risk awareness and supporting decision making in disaster risk reduction activities.

Keywords: Middle East; seismic risk; flood risk; multi-hazard risk

1. Introduction

Six active seismic zones bound the Arabian Peninsula in the Middle East: the Dead Sea Transform Fault, the Palmyra Fold Belt, the Zagros Fold Belt, the Red Sea and the Gulf of Aden Rift Spreading and the Makran Subduction Zone. The interaction of the Arabian Peninsula with the surrounding continents triggered several devastating events in the region. For example, the 1927 M6.3 Jericho earthquake in Palestine claimed about 300 lives and destroyed several cities (Elnashai and El-Khoury 2004). The 1956 M5.5 Chim earthquake in Lebanon triggered multiple shocks that killed nearly 135 people and destroyed 6 thousand homes (Elnashai and El-Khoury 2004). The 1982 M6.2 earthquake in Yemen killed 1,900 people and caused 153 million USD of economic losses (Ambraseys and Melville 1983). More recently, the M7.2 earthquake that hit Iran-Iraq borders in 2017 killed at least seven and injured another 500 people in Iraq (CRED 2019). Moreover, despite the aridity in the Middle East, several major floods affected the region (e.g., Mahmoud and Gan 2018). For example, the 2009 Jeddah flood in Saudi Arabia killed 160 people and caused damages of 900 million USD (CRED 2019). The 2008 Yemen flood killed 90 people and caused 400 million USD in losses (CRED 2019). The 2015 Iraq floods blocked the capitals' sewer system and killed 58 people (OCHA 2015).

The Global Assessment Report (GAR) for disaster risk reduction (UNDRR 2019) indicates that investments for disaster risk reduction (DRR) between 2005 and 2017 represented only 3.8% of the total investment, with the majority of the funds being used to support post-disaster response activities. From the perspective of political decision-makers, this investment gap is driven by the lack of knowledge and bias towards the benefits and costs of prevention and mitigation, which is primarily related to the scarcity of disaster risk information (e.g., Hugenbusch and Neumann 2016). As emphasized in the Sendai Framework for Disaster Risk Reduction 2015-2030 (SFDRR), DRR policies must be based on the knowledge of risk and, consequently, on its underlying components: exposure, vulnerability and hazard. In this context, exposure represents the characteristics of the elements at risk, vulnerability defines the susceptibility of those elements to suffer damage or loss, and hazard stands for the physical phenomena that cause ground shaking or flooding. Within this scope, the history of registered disasters is short and covers only limited regions. A review by UNISDR and EM-DAT (2018) indicates that about 63% of the documented disasters do not incorporate any information about the economic impact. These limitations in disaster data do not allow decision-makers to plan and implement disaster risk reduction measures based solely on information from past events. It is thus necessary to rely on catastrophe risk models that can provide relevant risk information to support risk management strategies. This immediate need has been highlighted in the main goals of the SFDRR.

One of the first probabilistic risk models covering the Middle East was developed as part of the Global Assessment Report (GAR 2015). The exposure model used by GAR was derived based on a top-down approach, where national/regional population and socio-economic data were used as a proxy to estimate building counts (De Bono and Chatenoux 2015). The seismic hazard component was developed using the NEIC-USGS earthquake catalogue and hundreds of seismic sources distributed across six tectonic regions (Ordaz et al. 2014). The flood hazard model relied on regional flood frequency analysis using stream-flow data for thousands of stations around the globe (Rudari et al. 2015). The vulnerability component relied on existing models for other regions that were applied to the Middle East. These datasets were used to estimate annualized average losses and aggregated losses for specific return periods. The major limitation of this risk assessment was the detail, vintage and applicability of the underlying components to this region. Moreover, the results were presented at the national level, thus preventing the support of decision-making at the sub-national level. To this end, an open-access and up-to-date regional model developed at the country level for the Middle East is fundamental for regional, national and local stakeholders. Quantifying the potential impact of natural hazards on portfolios of properties located in hazard-prone regions is of primary interest to property owners, (re-)insurance companies, capital lending institutions, local government agencies, and structural engineers. Each stakeholder is likely to have different requirements and contribute to disaster risk management using a variety of strategies (e.g., proactive structural retrofit, insurance coverage, catastrophe bonds). Regardless of which risk reduction or risk transfer mechanism is ultimately chosen, the estimates of potential losses on which these decisions are based must be as accurate as possible, given the available information.

To this end, this study estimates economic losses for the residential building stock in the Middle East (Jordan, Syria, Palestine, Saudi Arabia, Lebanon, United Arab Emirates, Yemen, Oman, Kuwait, Qatar, Bahrain and Iraq) due to earthquakes and floods. The country of Iran was not included herein, as it was part of another study already published (Motamed et al. 2019). The economic losses are calculated using recent seismic and flood hazard models, as well as high-resolution exposure data and vulnerability functions to reflect the diversity of construction types in the region. Earthquake losses are estimated using the event-based calculator of the OpenQuake-engine (Silva et al. 2014), while flood losses are derived from a simple convolution over a range of flood-depth hazard return periods. The results are presented in terms of the expected annualized loss and the probable maximum loss curves at the national and smallest available administrative level (i.e., region, province and municipality). Finally, the results are critically discussed and compared with similar studies/findings from the existing literature.

1.1 Previous efforts regarding risk modelling in the Middle East

The paucity of exposure, vulnerability and hazard information in the Middle East prevented the development of reliable catastrophe loss models for the region. For example, most exposure models usually cover only small regions and few building classes. Vulnerability studies, as illustrated in Yepes-Estrada et al. (2016), are mostly available for economically developed nations with moderate to high seismic hazard. Hazard information is often produced for drafting building codes, whereas probabilistic seismic hazard analysis (PSHA) models suitable for risk analyses remain unavailable or limited in terms of their scope and accuracy/detail.

The first risk study based on a probabilistic assessment for the Middle East was developed as part of the GAR, which provides loss estimates on a country basis worldwide. The Earthquake Model for the Middle East (EMME - Erdik et al. 2012) produced a harmonized seismic hazard model covering a region from Turkey to Pakistan, but it did not consider the Arabian Peninsula, and a probabilistic seismic risk assessment was not performed. Loss assessment studies at the local scale are rare and usually limited to specific areas. For example, Al-masni (2012) performed an earthquake scenario loss assessment for the residential buildings of Sana'a city in Yemen. Similarly, Al Shamsi (2013) estimated the economic and human losses based on an earthquake scenario for Dubai in the United Arab Emirates. Jaradat et al. (2008) estimated the economic losses due to an earthquake scenario for several facilities located in the greater municipality of Amman in Jordan. Makhoul et al. (2016) evaluated damage for several earthquake scenarios for Byblos in Lebanon. Studies concerning the estimation of economic losses due to floods seem to be inexistent for this region. Given the absence of local risk assessment studies, the added value of the proposed work is illustrated through a comparison with the GAR model and demonstrated in Table1. In this study, several efforts were undertaken to collect detailed data and develop customized models. In particular, the exposure component was developed on a country basis and incorporates additional data sources, such as census surveys and the judgment of local engineers. Moreover, the spatial resolution of the exposure datasets was improved using earth-observation datasets (Dabbeek and Silva 2020). Finally, the flood hazard spatial resolution and return periods are more detailed and also extend to flash flooding. It is worth mentioning that the GAR model detail differs from region to region, as explained in Cardona et al. (2015).

Table 1 Risk model features for the existing risk model in the literature and the proposed model.

Component	GAR[a]	This study
Exposure		
main data sources	Satellite, expert study	Census, satellite, community-based
max spatial resolution	Disaggregated at a 1 x 1 km^2	Disaggregated at a 38 x 38 m^2
Flood vulnerability		
geographical context	South America (CAPRA)	Asia (JRC)
Seismic vulnerability		
geographical context	USA (HAZUS)	Global (GEM)
Flood hazard		
flooding type	Riverine	Riverine, flash flooding
spatial resolution	1 x 1 km^2	90 x 90 m^2
mean return periods	six [b]	ten [c]

[a] only applies to countries investigated in this study; [b] 25, 50, 100, 200, 500, 1,000 years; [c] 5, 10, 20, 50, 75, 100, 200, 250, 500, 1,000 years

2. Methodology and description of risk components

2.1 Multi-hazard exposure model

Exposure models characterize the location, value and physical attributes of properties at risk. In this study, the exposure model from Dabbeek and Silva (2020) was adopted. This model was developed using national housing and population census surveys, existing literature and the feedback of local experts. It includes information on the number of buildings, dwellings and population with corresponding construction type, economic value, and geographical location. The construction typologies in the region are classified into 30 building classes distinguished by height, construction material, lateral-load resisting system, ductility level, and presence of basements (the latter being relevant for flood vulnerability assessment). Table 2 illustrates a summary of the main building types classified following the multi-hazard exposure taxonomy (Silva et al. 2018). In this model, replacement costs are distinguished by area (urban or rural) and construction quality, while accounting for the value of contents, structural and non-structural components. Built-up areas were estimated using building height, average dwelling size, and the average number of dwellings per floor. The exposure information is available at a 38x38 m^2 spatial resolution. The dataset comprises about 14.8 million buildings, with a cost of 1.23 trillion USD and 130 million inhabitants. Fig. 1 presents the number of buildings mapped at the lowest administrative level available for each country.

Table 2 Distribution of the common building typologies in the Middle East.

Building class	Buildings (thousand)	Buildings (%)	Buildings per class (%)	
			urban	rural
CR+CIP/LFINF+DUL/HBET:1-3	6,565	44.13	61.3	38.7
MCF+CBH/LWAL+DUL/HBET:1-2	1,160	7.80	52.0	48.0
MUR+CBH/LWAL+DUL/HBET:1-2	1,090	7.32	82.9	17.1
EU/HEX:1	980	6.59	15.5	84.5
CR+CIP/LFINF+DUL/HEX:1	900	6.05	55.1	44.9
MUR+STDRE/LWAL+DNO/HBET:1-2	795	5.34	37.9	62.1
MCF+CBH/LWAL+DNO/HBET:1-3	687	4.61	38.2	61.8
MATO/LN/HEX:1	456	3.07	51.6	48.4
CR+CIP/LFINF+DUL/HBET:1-3+HBEX:1	421	2.83	54.5	45.5

CR+CIP/LFINF+DUM/HBET:1-3	352	2.36	99.5	0.5
CR+CIP/LFINF+DUL/HEX:2	310	2.08	55.2	44.8
MCF+CLBRS/LWAL+DNO/HBET:1-2	263	1.76	18.2	81.8
MUR+STDRE/LWAL+DNO/HBET:1-3	209	1.40	94.8	5.2
MUR+ADO/LWAL+DNO/HEX:1	147	0.99	88.1	11.9
CR+CIP/LDUAL+DUL/HBET:4-7	121	0.82	93.6	6.4
CR+CIP/LFINF+DUL/HBET:4-7	79	0.53	92.5	7.5
W/HEX:1	52	0.35	23.5	76.5
CR+CIP/LFINF+DUL/HBET:4-7+HBEX:1	23.7	0.16	91.6	8.4

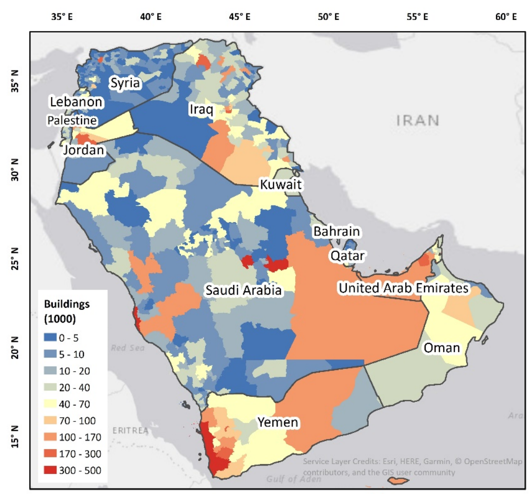

Fig. 1 Number of buildings at the smallest administrative level.

2.2 Vulnerability

2.2.1 Seismic fragility and vulnerability

As demonstrated in Yepes-Estrada et al. (2016), the Middle East is one of the regions in the world with the strongest lack of vulnerability models, with only a few studies in the past decades. A fragility model (i.e., likelihood of damage levels/states conditional on hazard intensity measures) was developed for the most common building types in Palestine (Grigoratos et al. 2016). Other efforts in the region are mainly dedicated to single buildings. For example, Yaseen et al. (2015) investigated the fragility of unreinforced concrete-masonry structures common in the Kurdistan region of Iraq. Issa and Mwafy (2014) proposed several fragility models for emergency facilities in the United Arab Emirates. Despite the importance of these studies, these models are building-specific and their use for regional risk analyses is questionable (i.e., due to the building-to-building variability within each building class). Moreover, existing studies do not cover all of the types of construction.

Given the lack of country-specific studies, vulnerability or fragility functions are often adopted from different regions. For example, Hancilar et al. (2018) employed HAZUS-based functions (FEMA 2014) to assess seismic risk for Muscat, Oman. Similarly, Al-masni (2012) utilized the same functions to assess seismic risk for Sana'a, Yemen. Although some buildings may follow the design regulations used in the United States (i.e., Uniform Building Code - UBC 1997; see Dabbeek and Silva 2020 for a review on the history of design codes in the Middle East), they are expected to behave differently, at least due to the different construction methodologies and code enforcement in the region. Another approach is to adopt functions from the closest neighboring country. For example, Makhoul et al. (2016) used fragility models from Turkey to assess risk for Byblos, Lebanon. The worldwide shortage of vulnerability and fragility functions, especially in developing countries, propelled several efforts. For example, GAR provides vulnerability functions for seismic risk assessment and other hazards based on the expert's judgment and published literature (Maqsood et al. 2014). Another recent effort led by the Global Earthquake Model (GEM) Foundation produced analytical fragility and vulnerability functions for the most common building typologies globally, including the typical buildings found in the Middle East (Martins and Silva 2020).

The vulnerability functions used in this study are selected from the GEM global vulnerability database (Martins and Silva 2020). The database comprises around 500 functions grouped by construction material, lateral load resisting system, ductility level and height. Ductility levels are separated into four categories to reflect different levels of seismic design as the following: low-ductility (DUL) for structures constructed pre-1960 or designed for low seismic demand (i.e., areas with low seismic hazard), medium-ductility (DUM) for structures that are compliant with some design regulations and built in areas with moderate seismic hazard, and high-ductility (DUH) for structures designed with modern building codes. In addition, a non-ductile (DNO) category was defined for unreinforced masonry, adobe and mud structures (which are typically the most vulnerable). In the development process described by Martins and Silva (2020), each building class has been represented by a single-degree-of-freedom (SDoF) oscillator characterized by the capacity spectrum relation (spectral displacement - Sd vs spectral acceleration - Sa). Then, each oscillator was subjected to nonlinear dynamic analysis using a database of 3500 ground motion records that consider a range of magnitudes, distances and tectonic environments (including active shallow regions relevant for the Middle East). After the nonlinear time history analysis, the response (in terms of spectral displacement) was classified into four damage states using the thresholds illustrated in Table 3. For each damage state, a fragility curve is fitted using the procedure proposed by Jalayer et al. (2015). Two fragility functions are presented for two of the most common building classes in Fig. 2a and 2c. Each of the fragility functions is converted into a vulnerability function using a consequence model (also known as damage-to-loss model), in which the probability of being in a particular damage state is multiplied by the associated mean loss ratio (see Table 3), the loss ratio is defined here as the percentage of the cost of repair to the cost of replacement. The resulting vulnerability functions for the same building classes are presented in Fig. 2b and 2d.

Table 3 Damage states thresholds and corresponding loss ratio (adapted from Martins and Silva 2020).

Damage category	Damage thresholds	Mean loss ratio (%)
Slight	0.75 Sdy	5
Moderate	0.5 Sdy + 0.33Sdu	20
Extensive	0.25 Sdy + 0.67 Sdu	60
Complete	Sdu	100
Sdy and Sdu stand for the yielding and ultimate spectral displacement		

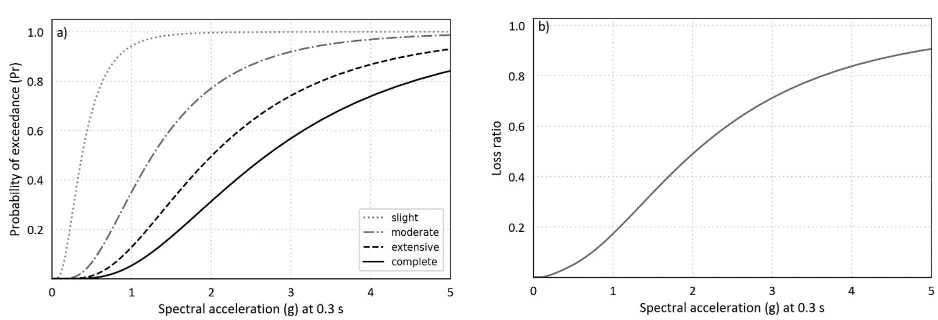

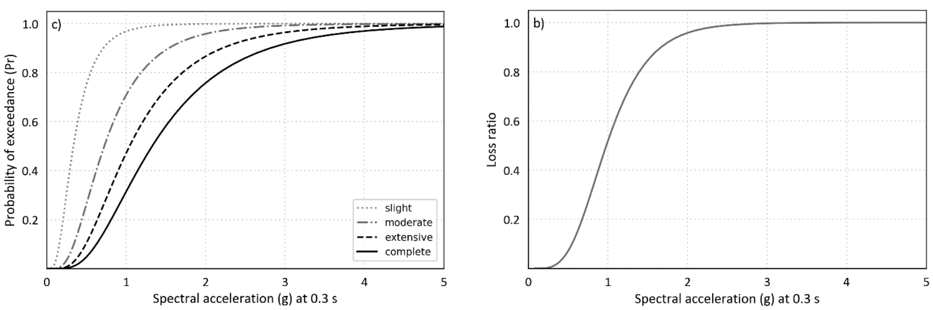

Fig. 2 Fragility (a) and vulnerability (b) functions for a low-ductility, two-story reinforced concrete infilled frame, fragility (c) and vulnerability (d) functions for a non-ductile, one-story, unreinforced masonry (adobe).

2.2.2 Flood vulnerability

No vulnerability or damage data was found for the region covered by this study. Thus, a vulnerability model was selected amongst several existing studies for other regions, and then further adapted to better represent the characteristics of the built environment in the region.

I. Selection of flood vulnerability functions

The transferability of vulnerability models from one region to another depends on the characteristics of the model. In particular, the derivation method is one critical attribute that has to be considered. Often, damage models for floods are grouped into empirical (derived from observed post-event data), synthetic (expert-based using what-if analysis), or a mixture of both (i.e., Dottori et al. 2016). Other more complex procedures rely on analytical models to simulate force actions on buildings (i.e., hydro-static and hydro-dynamic pressure, debris impacts – e.g., Jalayer et al. 2015). Empirical methods are generally the most used in practice (Gerl et al. 2016). However, there are several challenges related to the transferability of these models to other regions. The limitations of using empirical methods are mitigated in this study by adopting functions developed for the same continent. Another attribute that has to be considered is the flood type and flood characteristics (i.e., depth, velocity, duration, contamination, and sediments), as they are directly related to building damage. For example, dam-break flooding is known to be abrupt and short, while river flooding can be slower and longer in duration. Given the flood types considered here, only fluvial and pluvial vulnerability functions were selected.

Other considerations that should support the selection of suitable fragility/vulnerability models for flood are related to building stock characteristics. For example, the occupancy (e.g., residential, commercial, industrial) influences the value of building contents (e.g., furniture, machinery, equipment) and non-structural elements (electrical, HVAC systems, finishes), which are the first to be damaged in case of direct contact with water. In this study, only the vulnerability functions developed for the residential sector were considered. Furthermore, the unit of analysis (i.e., building versus geographical area) should be consistent with the exposure characteristics (Merz et al. 2010). Similarly, if the damage scale is absolute (i.e., losses in USD), transferability becomes an issue. In contrast, a standardized damage scale (i.e., % of the building value) offers the possibility to reuse functions regardless of the economic disparities. Finally, it is also relevant to consider the physical characteristics of the buildings under consideration. In the selection process, we considered functions that can accurately characterize the vulnerability of the building stock given the construction material, age, number of floors and the presence of basements. A review of flood actions on buildings can be found in Kelman and Spence (2004).

Following these principles, the selection process considered a database composed of 47 vulnerability models compiled by Gerl et al. (2016), which was complemented with recently released models collected by the authors. As a result, the global flood depth-damage functions proposed by the Joint Research Center (JRC) of the European Commission were selected (Huizinga et al. 2017). These functions were developed empirically for different continents (e.g., Europe, Asia, Africa) and consider residential, commercial and industrial occupancies at the building level. We adopted the damage functions for the

Asian continent, which were then improved considering the building stock in the Middle East and the recommendations from the JRC and HAZUS (FEMA 2019), as described in the following sections.

II. Adaptation of flood vulnerability functions

The JRC’s vulnerability functions are generic, while the building stock considered in this study has heterogeneous physical characteristics. For this reason, the following two steps were used to adjust the original functions considering the main types of construction material and heights:

a. The adjustment of the vulnerability functions considering different construction materials and content value is done following the JRC recommendations. In particular, a 60% maximum damage is considered for reinforced concrete and masonry buildings. This damage threshold is also in agreement with the HAZUS guidelines. It is important to note that both models (JRC and HAZUS) consider that contents represent 50% of the total building value. However, the value of contents in the Middle East is significantly lower (between 20-30%). The total maximum damage was set to 45% of the total building value, to avoid an overestimation of the losses, which is also consistent with the maximum damage threshold used by the GAR global flood vulnerability model (Maqsood et al. 2014). For non-resilient materials (i.e., mud, adobe and rubble-stone), the maximum damage is set to 100% as recommended by the JRC guidelines.

b. The vulnerability functions were also adjusted to account for the different building heights. The JRC's database of vulnerability functions does not provide the individual functions used to construct the generic models nor the contribution of each height category. To adjust the original functions based on the height, we used the HAZUS vulnerability functions, which define damage by height category. In this process, the HAZUS damage ratios for one, two and three stories are averaged, as shown in Equation (1). Then, the contribution of each height relative to the average damage is computed, as shown in Equation (2). In the last step, this value is multiplied by the JRC function (after adjusting for material and content) to obtain the damage per building height as illustrated in Equation (3).

$$\bar{D}_{i\,(hazus)} = \frac{d_{i,1} + d_{i,2} + d_{i,n}}{n} \qquad i\,(depth) = \{0,6\} \tag{1}$$

$$c_{\,i,n} = \frac{d_{i,n}}{\bar{D}_{i\,(hazus)}} \tag{2}$$

$$d_{i,n\,(adapted)} = c_{\,i,n} \times \bar{D}_{i\,(jrc)} \tag{3}$$

Where $d_{i,n}$ stands for the damage ratio at the hazard intensity (*i*) for building (*n*), $\bar{D}_i$ represents the average damage ratio of all heights. $c_{i,n}$ refers to the relative difference between the damage ratio for a single building to the average of all buildings. In should be noted that at a given intensity, when the building height doubles (from one to two stories), the damage does not decrease proportionally. Typically, the distribution of building value is uneven across building floors (i.e., it is common that the central electrical and mechanical units are installed in the basement or ground floor). Fig. 3 illustrates the damage ratio given flood-depth after adjustment, for one- and two-story reinforced concrete buildings.

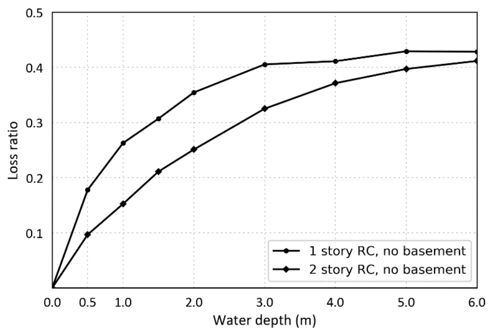

Fig. 3 Flood vulnerability for one and two stories RC building.

2.3 Hazard

2.3.1 Seismic hazard

The Middle East is one of the most seismically active regions in the world (Ambraseys and Melville 1983; Zare et al. 2014). However, there is a misleading assumption about the low seismicity of the Arabian Peninsula due to the absence of events in the 20th century, particularly after the improvement of the worldwide seismological network in the 1960s (Ambraseys and Melville 1983). Arabia had a long history of seismic activity with several devastating earthquakes (Ambraseys et al. 1994). Recently, Zare et al. (2014) compiled a catalogue for earthquakes between 1250 B.C. to 2006 based on historical reviews (e.g., Ambraseys et al. 1994; Ambraseys 2009) and recent instrumental records, as presented in Fig. 4. As previously discussed, the seismicity in Arabia is a result of the convergence motion with Eurasia in East-Turkey and Iran, and the Africa-Arabia spreading in the Red Sea. The seismic hazard of the tectonic regions bounding Arabia has been the target of several studies. The Dead Sea Fault system and the Palmyra Fold Belt hazard affecting Lebanon, Syria, Palestine, Jordan and North Saudi Arabia has been investigated by Elnashai and El-Khoury (2004), El Ssayed et al. (2012), Al-Homoud and Husein (1995), and Al-Arifi et al. (2013). The seismicity around the Red Sea and Golf of Aden affecting Saudi Arabia and Yemen has been studied by Zahran et al. (2015) and Mohindra et al. (2012). The Biltis-Zagros belt and Makran subduction affecting Iraq, United Arab Emirates, Kuwait and Oman are documented in Pascucci et al. (2008), Abdalla and Al-homoud (2004), and Farman and Said (2018).

Other regional and global seismic hazard programs for the Middle East include the Seismotectonic and Seismic Hazard Assessment of the Mediterranean Basin (SESAME- Jiménez et al. 2001) and The European Seismological Commission Working Group on Seismic Hazard Assessment (ESC/WGSHA - Jimenez et al. 2003). At the global level, the first seismic hazard map was developed within the Global Seismic Hazard Assessment Program (GSHAP- Giardini 1999). More recently, another seismic hazard map for the region was created within the framework of the Global Assessment Report (GAR - Ordaz et al. 2014).

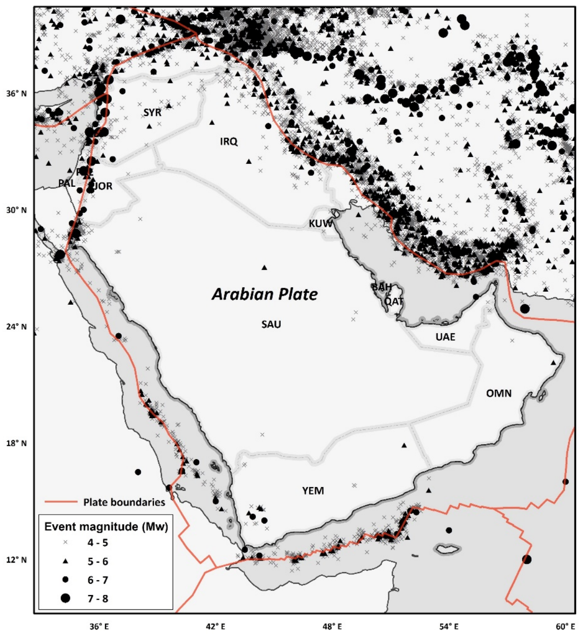

Fig. 4 Earthquake catalog developed within the scope of the Earthquake Model for the Middle East project (adapted from Zare et al. 2014).

At the regional scale, a probabilistic seismic hazard model was proposed for the northern countries of the Middle East (Danciu et al. 2018) as part of EMME project, and similarly for Southern Arabia by Sokolov et al. (2017). These models incorporate a unified instrumental and historical catalogue, as well as a comprehensive active faults database for the region. The seismogenic source model is structured in two possible sources (areal and fault). Each source is classified according to its tectonic regime (i.e., stable, active, subduction and deep seismicity). Then, for each tectonic regime, one or multiple ground-motion models (GMMs) are combined using logic trees. These two models were implemented in the OpenQuake-engine (Pagani et al. 2014), as part of the global hazard model (Pagani et al. 2020) initiative led by the GEM Foundation. Fig. 5 presents the seismic hazard in the studied region in terms of peak ground acceleration (PGA) for a 10% probability of exceedance in 50 years considering rock conditions (V_{S30} = 760 m/s). Dabbeek and Silva (2020) estimated that about 27% of the total population (i.e., 165 million) is exposed to a moderate-to-high seismic hazard (PGA above 0.15 g for the 10% probability of exceedance in 50 years on rock).

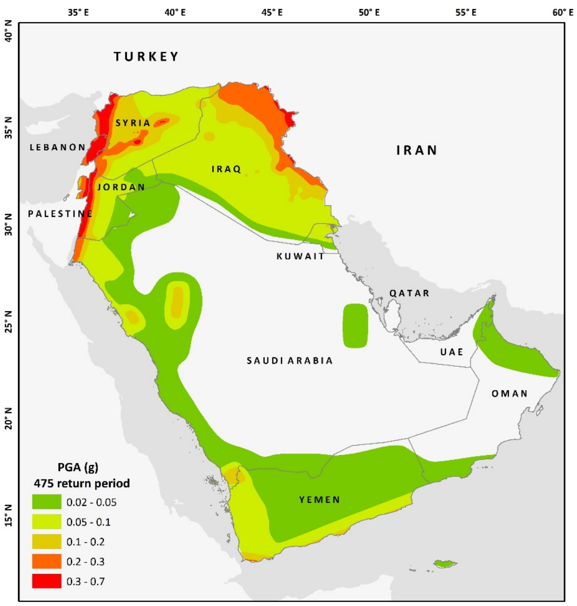

Fig. 5 Seismic hazard map for the Arabian Peninsula (PGA for 10% probability of exceedance in 50 years).

2.3.2 Flood hazard

Arid and semi-arid environments are commonly subjected to sporadic storms of high spatial and temporal variability (Al-Wishah 2002). These climatic interactions combined with the lack of vegetation in a dry climate, watershed properties, human interference in the form of land-use change and the inadequate water control systems can intensify flood generation (Wheater, 2002; Mahmoud and Gan 2018). The hydrology of arid and semi-arid regions is thoroughly described in ŞEN (2008). For the current application, we used the high-resolution global flood hazard model proposed by Sampson et al. (2015). This model accounts for both river and flash flood inundation, and it allows estimating discharge for small channels (catchments smaller than 50 km^2). Moreover, it is a true hydrodynamic flood model, explicitly simulating flood wave propagation using a 2D shallow-water formulation (Bates et al. 2010). Lastly, since input data in developing countries is limited (for a discussion see Galasso and Senarath 2014), river discharge is estimated with a method that allows transferring data from data-rich countries to poorer nations (Smith et al. 2015). This methodology does not use a cascade hydrological modelling approach to derive discharge, but instead uses a regionalized flood frequency analysis, linking extreme flow behaviour to upstream catchment characteristics. Therefore, discharge is estimated by identifying the upstream catchment characteristics for any river channel cell. Furthermore, the model employs different filtering techniques to correct elevation data bias caused by dense vegetation and urbanization. In addition to fluvial flooding, the model framework also simulates pluvial inundation by 'raining' directly onto the simulated digital elevation model and the underlying channel structures. The model employs a sub-grid channel network that, as mentioned previously, explicitly simulates in channel flow for all channels regardless of size (Neal et al. 2012). This sub-grid channel network is also in-place for the pluvial simulations and allows excess rainfall to be conveyed and floodplain drainage behaviour to be appropriately simulated. Channel bathymetry is defined using the estimates of discharge derived from the regionalised flood frequency analysis, with channel bathymetry being linked to a given return-period flow (e.g. the channel can convey the 1 in 2-year flow). The implementation of small-scale local drainage features was not considered. Fig. 6 shows an example of a flood hazard map for Iraq and a section of the Tigris river, with water depth corresponding to the 100-year return period at a resolution of 90x90 m^2. Dabbeek and Silva (2020) estimated that about 10% of the population in the region (i.e., 165 million) is exposed to moderate-to-high flood hazard (water depth above 30 cm for the 100-year return period).

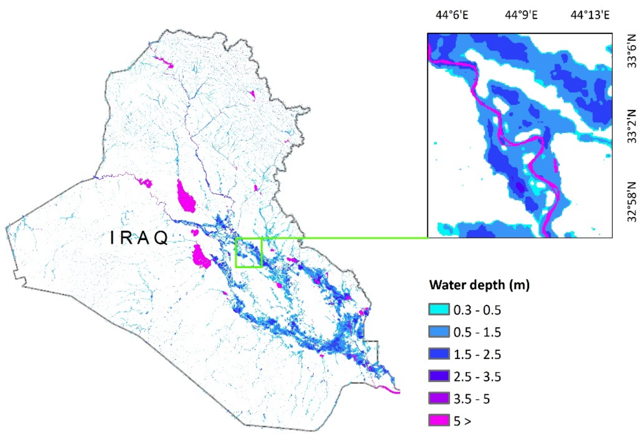

Fig. 6 Flood hazard map expressed in terms of water depth for the 100-year return period for Iraq and a section of Tigris river (adapted from Sampson et al. 2015).

3. Risk results

3.1 Seismic risk

The economic losses due to seismic hazard were derived using the event-based calculator of the OpenQuake-engine (Silva et al. 2014). In this approach, events are sampled over a specific period using a Monte Carlo sampling procedure to generate a stochastic event set (SES). For this application, 30,000 SESs with a 1-year duration were generated. For each event, the ground shaking in the region was estimated using the GMMs used in the regional hazard models discussed above. The results at a particular site are used to estimate the annual rate of exceeding a set of ground shaking levels, commonly known as a seismic hazard curve. Furthermore, the ground shaking was combined with the vulnerability functions to determine building damage/loss. When applied to the entire SES, the likelihood of exceeding a set of loss levels is known as the loss exceedance probability (*EP*) curve. The relation between the absolute losses and the return periods represents the probable maximum loss curve illustrated in Fig. 8. This curve can also be converted into an *EP* curve by converting each return period to an annual rate of exceedance (i.e., the inverse of the return period). It is recognized that probabilities and rates are distinct, but for a 1-year time span, these two variables are practically identical. The total losses generated by the SESs can be summed and divided by the number of SESs, leading to the average annualized loss (*AAL*). Fig. 7 presents a summary of the absolute and relative *AALs* (loss normalized by buildings replacement value) by country. The results indicate an *AAL* of 323 million USD at the regional level, with the highest absolute losses in Syria, Iraq and Lebanon. When normalized, the highest values are observed in Lebanon, Syria, and Jordan. The lowest losses are located in Bahrain and Qatar. Notably, although the expected losses for Syria are higher than Lebanon, the probable maximum loss curve in Fig. 8 indicates that rarer events (i.e., higher than 100-year return period) are expected to cause higher losses in Lebanon.

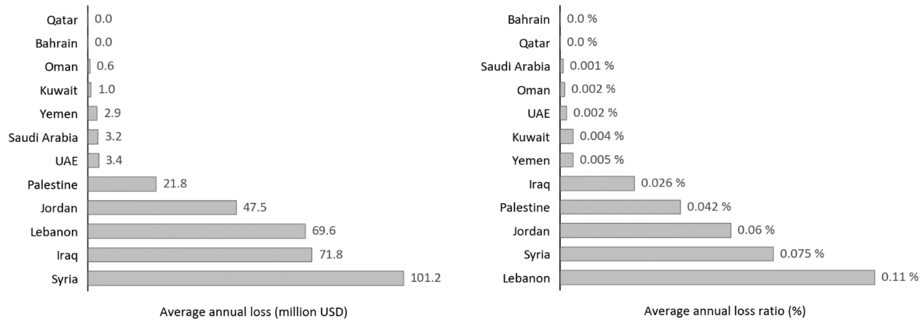

Fig. 7 Average annual losses (left) and average annual loss ratios (right) due to seismic hazard.

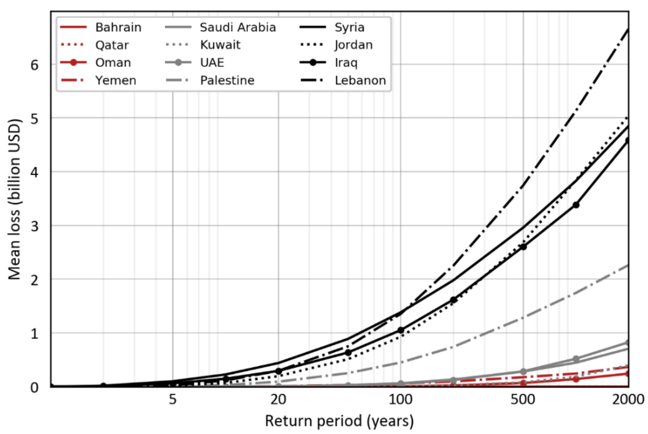

Fig. 8 Probable maximum losses.

3.2 Flood risk

The results for flood risk were also expressed in terms of *AALs*. However, unlike the approach followed in estimating seismic risk, generating full stochastic event sets for flood hazard is quite computationally demanding. Instead, ten hazard maps for return periods of 5, 10, 20, 50, 75, 100, 200, 250, 500 and 1,000 years were used for the flood loss assessment. The water depth at the location of each building was combined with a vulnerability model to calculate the loss ratio corresponding to each return period. The set of loss ratios were then converted into a set of absolute losses by multiplying each loss ratio by the building replacement cost. The *AAL* is obtained by estimating (or numerically integrating) the area under the *EP* curve. The accuracy of this estimation depends on the number of return periods (or rates of exceedance). Messner et al. (2007) proposed using at least three return periods to estimate the *AAL*. Similarly, Ward et al. (2011) found that the choice of bounds and the number of return periods influence risk estimates. In particular, the study demonstrated that disregarding frequent events (i.e., bellow the 10-year return period) underestimated the annual average losses by 30%. The study also demonstrated that the average annual losses are not significantly affected by return periods longer than 1,000 or 2,000 years. In this study, a range between the 5-year and the 1,000-year return periods was considered. Another factor of uncertainty regards the relationship between the elevation of the surrounding land and the elevation of the first floor. To avoid an overestimating of the losses, a 0.2 m threshold was assumed, as suggested for the residential sector in several studies (e.g., Maqsood et al. 2014; Olsen et al. 2015). Unlike what was presented for the seismic risk counterpart, for flood risk, it was not possible to derive exceedance probability curves at the national level due to the fact that hazard maps were used for the loss calculations and not large sets of stochastically generated events.

Fig. 9 presents the results for flood risk in terms of the expected *AAL*. These results suggest that Iraq and Syria have the highest losses in both absolute and relative terms. This correlation between the two metrics emphasizes the high population density and vulnerability of buildings within the flood plains of the Tigris and Euphrates rivers (i.e., the average annual loss ratio for Iraq is almost 0.19%). The high losses in Saudi Arabia and Yemen represent only 0.01% and 0.018% of the exposed value. This highlights the profound localized impacts of flash floods in major urban areas such as Jeddah and Sana'a.

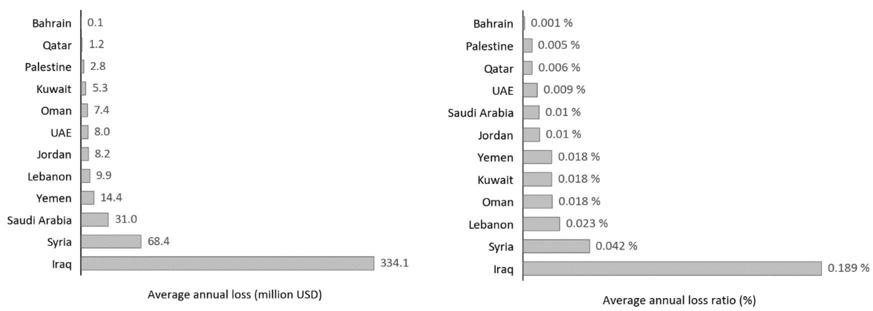

Fig. 9 Floods expected average annual loss (left), average annual loss ratio (right).

3.3 Multi-hazard risk

Floods and earthquakes are independent events, and consequently, the total annualized risk can be estimated by summing the respective *AALs*. We note however that for rare return periods, it is plausible to have damaging earthquakes and floods occurring in the same year. Fig. 10 illustrates the distribution of total losses aggregated at the smallest administrative boundaries. The results indicate that the largest losses are located in Syria and Iraq. Moreover, it can be noted that at the sub-national scale, some regions are subjected only to flood or seismic risk.

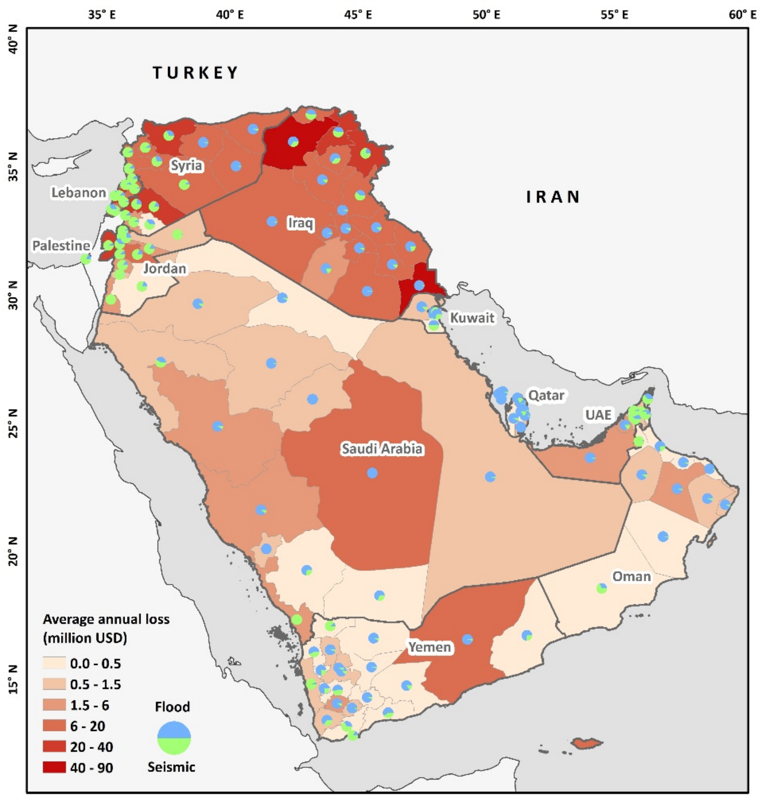

Fig. 10 Spatial distribution of average annual losses due to seismic and flood hazard in the Middle East.

4. Discussion of the results

The estimated losses were first compared with observed data and then with other exiting models. The aim was to verify whether the combination of risk components provides reasonable estimates consistent with past observations and the existing literature. Other tests using data from past events is described at the global scale in Silva et al. (2020) . Some insights are also provided regarding the adopted models and their influence on the results.

Deleted:

4.1 Comparing seismic risk results with the literature

Historical loss data are usually poor in terms of their quality, quantity and level of aggregation. Thus, earthquake loss results are compared only with the GAR model. Table 4 presents a comparison between the proposed model and the GAR results. There is a reasonable agreement between both models for the Levant countries (Palestine, Jordan, Syria and Lebanon) close to the Dead Sea Fault, with slightly higher values predicted by the model proposed herein. For the remaining countries, the model predicts considerably different results, with the GAR model in general reporting higher losses. In particular, the differences observed between the two models for Yemen, Iraq and United Arab Emirates are mostly due to the striking differences in the hazard component. The hazard used in this study is presented in Fig. 5, while GAR's hazard map for the same probabilities can be found in Ordaz et al. (2014). In Yemen, the hazard map for GAR indicates a PGA of up to 0.3 g for the 10% probability of exceedance in 50 years in densely populated regions, while the model used in this study presents lower values, in the order of 0.2 g along the seashores of Yemen, which are less populated than the central region. In the United Arab Emirates, the seismic hazard used within GAR indicates values of up to 0.4 g in the eastern part of the country where most of the population live, whereas the model used in this study suggests much lower hazard values (below 0.1 g). A local study (i.e., Abdalla and Al-homoud 2004) discusses that the high hazard values often reported for the United Arab Emirates are grossly over-conservative. In Iraq, the values are comparable, yet the GAR's hazard footprint covers larger areas, including the capital city Baghdad. In contrast, the hazard used in this study is narrowed to the boundary regions. There is a clear disagreement in the hazard values in southern Arabia, which becomes evident in the risk estimates due to the population distribution.

Table 4 Comparison between the seismic loss estimates proposed by GAR and the proposed model.

Country	GAR model		This study	
	AALR (%)	*AAL* (millions)	*AALR* (%)	*AAL* (millions)
Lebanon	0.060	57.0	0.110	69.6
Syria	0.070	40.0	0.075	101.1
Jordan	0.040	15.1	0.060	47.5
Palestine	0.040	11.0	0.042	21.7
Iraq	0.120	46.5	0.026	71.8
Kuwait	0.043	**152.1**	0.004	1.0
Yemen	0.060	22.6	0.005	2.9
Bahrain	0.025	**18.0**	0.000	0.0
Oman	0.020	**35.0**	0.002	0.6
Saudi Arabia	0.008	**30.0**	0.001	3.2
Qatar	0.020	**86.1**	0.000	0.0
UAE	0.059	**572.0**	0.002	3.4

The second major difference is attributed to the allocated building classes. The GAR model utilizes the building fractions proposed by the Prompt Assessment of Global Earthquakes for Response (PAGER) group of the United States Geological Survey (Jaiswal et al. 2010). Table 5 compares the macro building classes utilized in both models per country. Both models agree that reinforced concrete is the most common construction type in the Middle East, but there are some clear discrepancies for some of the countries, as highlighted in Table 5. For example, PAGER considers buildings in Yemen as 100% composed of reinforced concrete which does not agree with the recent national census or other published literature. Furthermore, the high percentage of adobe buildings (60% and more) assigned to Iraq, Kuwait, Lebanon and Syria does not seem reasonable according to the feedback of the local experts. Surprisingly, masonry buildings are either too high (i.e., 70% for Palestine, Jordan and Bahrain) or too low. These differences can be explained by the fact that the PAGER model defined the building classes in the Middle East mostly based on an expert study from 1983 (Petrovski 1983).

Table 5 Comparison between the proposed model and GAR building classes.

Country	RC		Masonry		Adobe/Earthen	
	This study	GAR model	This study	GAR model	This study	GAR model
Bahrain	84%	9%	10%	**85%**	5%	5%
Iraq	45%	20%	47%	0%	8%	**80%**
Jordan	58%	30%	38%	**70%**	4%	0%
Kuwait	69%	1%	20%	46%	6%	**53%**
Lebanon	51%	40%	41%	0%	8%	**60%**
Oman	63%	100%	23%	0%	5%	0%

Palestine	47%	30%	45%	**70%**	5%	0%
Qatar	85%	100%	10%	0%	0%	0%
Saudi Arabia	68%	100%	20%	0%	0%	0%
Syria	44%	40%	41%	0%	10%	**60%**
UAE	85%	100%	10%	0%	0%	0%
Yemen	30%	**100%**	45%	0%	19%	0%

4.2 Comparing flood risk results with literature

The flood risk results were compared with empirical *AAL* derived from the International Disaster Database (EMDAT - CRED 2019), which covers a period between 1954 (first recorded event in the studied countries) and 2019, as well as the results from GAR (see Table 6). It should be noted that the EMDAT database comprises a total of 95 events, of which only 30 have declared economic losses. Clearly, the number of historical records is not statistically sufficient to estimate a precise empirical *AAL*, and thus the comparisons performed here are merely indicative.

The results demonstrate a reasonable agreement between the model proposed in this study and the other models (GAR and EMDAT). However, it is important to emphasize some caveats in the comparison. The estimated *AAL* for Iraq is about 334 million USD, while the empirical *AAL* is less than a million USD. This is due to the fact that many past events are listed in the EM-DAT database without any economic loss, despite the clear impact reported in media reports. Moreover, GAR estimates an *AAL* of 344 million USD, which is remarkably close to the value presented in this study. A similar observation stands for Syria for the relative *AAL* (0.056% and 0.050%), but GAR indicates a higher *AAL*, which suggests a higher estimation of the value of building stock. It should be noted that GAR does not consider flash floods, and thus no losses are predicted for the remaining countries as there are no major streams as in Syria or Iraq. For Yemen, the recorded losses are considerably higher than the estimated *AAL* from this study. This discrepancy is possibly due to the vulnerability function assigned to the stone buildings (which are quite popular in this country), which seem to underestimate the economic losses. Saudi Arabia is another country that has a long history of flash floods with 15 recorded events in the last decades and an observed *AAL* of 32 million USD. The *AAL* estimated in this study is relatively close to this value (i.e., 31 million USD). Oman is a particular case, as the observed *AAL* of 126 million USD is mostly due to cyclones, which are not considered here. Jordan, Palestine, Lebanon, Kuwait and United Arab Emirates have higher estimated losses than the recorded ones. However, no economic damages were reported for some events in the EMDAT. Bahrain and Qatar did not experience any major flood events, which is consistent with the estimates presented herein.

Table 6 Comparison between different flood risk estimates, EMDAT loss database, GAR model and proposed model.

Country	**EMDAT**	**GAR model**		**This study**	
	AAL (millions)	*AAL* (millions)	*AALR* (%)	*AAL* (millions)	*AALR* (%)
Iraq	0.9	**344.3**	0.260	**334.1**	0.121
Syria	0.9	114.7	0.056	68.4	0.050
Yemen	62.3	0.0	0.000	15.0	0.024
Kuwait	0.0	0.0	0.000	5.4	0.023
Oman	126.2	0.0	0.000	7.4	0.018
Lebanon	2.6	8.1	0.004	9.0	0.016
Jordan	0.7	3.0	0.002	8.2	0.010
Saudi Arabia	**32.1**	0.0	0.000	**31.0**	0.010
Palestine	0.0	0.3	0.000	2.8	0.005
UAE	0.0	0.0	0.000	8.0	0.005
Qatar	0.0	0.0	0.000	1.2	0.004
Bahrain	0.0	0.0	0.000	0.1	0.001

5. Conclusions and final remarks

This study presents a probabilistic loss assessment for earthquakes and floods in the Middle East. The results include average annual losses at national and subnational scales and loss exceedance curves at the national scale for earthquake risk. Both seismic and flood risk are significant within the studied region (i.e., *AAL* of 323 and 490 million USD, respectively), with the highest total losses in Iraq and Syria. In fact, although flood annualized losses exceeded the seismic counterpart, the distribution of losses showed that seismic risk is distributed across several countries in the region, while flood risk is more localized (i.e., mostly in Syria and Iraq).

It is important to recognize the caveats in this study prior to using any results. For the exposure component, the information corresponds to the latest available census, but some countries do not have up-to-date information (i.e., the latest census of Syria is from 2004), as discussed in Dabbeek and Silva (2020). For the flood risk assessment, this study used the closest neighbour vulnerability functions (i.e., Asian continent), which were further adjusted based on the building stock characteristics. However, there are several constraints in transferring empirical vulnerability from the context they were developed to other regions. For flood hazard, the model does not include protective measures such as dams and embankments, and therefore lower losses could be expected, at least due to events with lower return periods. On the seismic risk side, this study did not consider the impact of secondary hazards (e.g., landslides, liquefaction, tsunami and fires). In addition, floods triggered by tropical cyclones (i.e., affecting Yemen and Oman) were not considered. Despite the model limitations, the current work provides a comprehensive overview of the major risks in the Middle East, which could support sustainable planning, raising risk awareness, and inform investments for disaster risk reduction.

References

Abdalla JA, Al-homoud A (2004) Earthquake Hazard Zonation of Eastern Arabia. In: 13th World Conference on Earthquake Engineering (13WCEE). Vancouver, Canada

Al-Arifi NS, Fat-Helbary RE, Khalil AR, Lashin AA (2013) A new evaluation of seismic hazard for the northwestern part of Saudi Arabia. Nat Hazards 69:1435–1457. https://doi.org/10.1007/s11069-013-0756-1

Al-Homoud AS, Husein AI (1995) Probabilistic assessment of seismic hazard of dam sites in Jordan. Nat Hazards 11:123–134. https://doi.org/10.1007/BF00634529

Al-Masni MA (2012) Earthquake Building Risk Assessment in Sana'a City, Yemen. Asian Disaster Reduction Center (ADRC). https://www.adrc.asia/aboutus/vrdata/finalreport/2012A_YEM_fr.pdf. Accessed 24 Apr 2019

Al-Shamsi GA (2013) Seismic Risk Assessment of Buildings in Dubai, United Arab Emirates. American University of Sharjah

Al-Wishah RA (2002) Rainfall-Runoff analysis and modeling in wadi systems. In: Hydrology of wadi systems, IHP-V, Technical documents in hydrology 55. Paris, pp 87–111

Ambraseys N (2009) Earthquakes in the Mediterranean and Middle East. Cambridge University Press, Cambridge

Ambraseys NN, Melville CP (1983) Seismicity of Yemen. Nature 303:321–323. https://doi.org/10.1038/303321a0

Ambraseys NN, Melville CP, Adams RD (1994) The Seismicity of Egypt, Arabia and the Red Sea. Cambridge University Press, Cambridge

Bates PD, Horritt MS, Fewtrell TJ (2010) A simple inertial formulation of the shallow water equations for efficient two-dimensional flood inundation modelling. J Hydrol 387:33–45. https://doi.org/10.1016/j.jhydrol.2010.03.027

Cardona OD, Bernal GA, Ordaz MG, Salgado-Gálvez MA, Singh SK, Mora MG, Villegas CP (2015) Update on the probabilistic modelling of natural risks at global level: Global Risk Model. Prepared for the Global Assessment

Report on Disaster Risk Reduction 2015. Barcelona-Bogotá

CRED (2019) EM-DAT: The Emergency Events Database. https://www.emdat.be/. Accessed 17 Jul 2018

Dabbeek J, Silva V (2020) Modeling the residential building stock in the Middle East for multi-hazard risk assessment. Nat Hazards 100:781–810. https://doi.org/10.1007/s11069-019-03842-7. https://github.com/jamaldabbeek/Exposure-data

Danciu L, Kale Ö, Akkar S (2018) The 2014 Earthquake Model of the Middle East: ground motion model and uncertainties. Bull Earthq Eng 16:3497–3533. https://doi.org/10.1007/s10518-016-9989-1. http://www.efehr.org/en/Documentation/specific-hazard-models/middle-east/hazard-computation-input/

De Bono A, Chatenoux B (2015) A Global Exposure Model for GAR 2015. UNEP/GRID-GENEVA, UNISDR. Geneva, Switzerland

Dottori F, Figueiredo R, Martina ML V., Molinari D, Scorzini AR (2016) INSYDE: a synthetic, probabilistic flood damage model based on explicit cost analysis. Nat Hazards Earth Syst Sci 16:2577–2591. https://doi.org/10.5194/nhess-16-2577-2016

El Ssayed HM, Zaineh HE, Dojcinovski D, Mihailov V (2012) Re-Evaluations of Seismic Hazard of Syria. Int J Geosci 03:847–855. https://doi.org/10.4236/ijg.2012.324085

Elnashai AS-E, El-Khoury RR (2004) Earthquake Hazard in Lebanon. Published by Imperial College Press and Distributed by World Scientific Publishing Co.

Erdik M, Sesetyan K, Demircioglu MB, Tüzün C, Giardini D, Mansouri B, Lodi S, Al-nimry H, et al (2012) Seismic Risk Assessment in the Middle East and EMME (Earthquake Model of Middle East) Project. In: 15th World Conference on Earthquake Engineering (15WCEE). Lisboa

Farman MS, Said AI (2018) Updated Probabilistic Seismic Hazard Assessment for Iraq/2018. Civ Eng J 4:1610. https://doi.org/10.28991/cej-0309199

FEMA (2014) HAZUS-MH MR5, Technical Manual, Department of Homeland Security - Federal Emergency Management Agency. Washington, D.C.

FEMA (2019) HAZUS-MH MR3 Technical Manual, Multi-hazard Loss Estimation Methodology, Flood Model. Washington, D.C.

Galasso C, Senarath SUS (2014) A Statistical Model for Flood Depth Estimation in Southeast Europe. Vulnerability, Uncertainty, Risk 1415–1424. https://doi.org/10.1061/9780784413609.142

GAR GAR (2015) UNISDR 2015 Global Assessment Report. https://www.preventionweb.net/english/hyogo/gar/2015. Accessed 26 Mar 2020

Gerl T, Kreibich H, Franco G, Marechal D, Schröter K (2016) A Review of Flood Loss Models as Basis for Harmonization and Benchmarking. PLoS One 11:e0159791. https://doi.org/10.1371/journal.pone.0159791

Giardini D (1999) The Global Seismic Hazard Assessment Program (GSHAP) - 1992/1999. Ann Geophys 42:. https://doi.org/10.4401/ag-3780

Grigoratos I, Dabeek J, Faravelli M, Di Meo A, Cerchiello V, Borzi B, Monteiro R, Ceresa P (2016) Development of A Fragility and Exposure Model for Palestine – Application to The City of Nablus. Procedia Eng 161:2023–2029. https://doi.org/10.1016/j.proeng.2016.08.797

Hancilar U, El-Hussain I, Sesetyan K, Deif A, Cakti E, Al-Rawas G, Safak E, Al-Jabri K (2018) Earthquake risk assessment for the building inventory of Muscat, Sultanate of Oman. Nat Hazards 93:1419–1434. https://doi.org/10.1007/s11069-018-3357-1

Hugenbusch D, Neumann T (2016) Cost-Benefit analysis of disaster risk reduction: A synthesis for informed decision making. Bon, Germany

Huizinga J, de Moel H, Szewczyk W (2017) Global flood depth-damage functions: Methodology and the database with guidelines. EUR 28552 EN. doi: 10.2760/16510. https://ec.europa.eu/jrc/en/publication/global-flood-depth-damage-functions-methodology-and-database-guidelines

Issa A, Mwafy A (2014) Fragility Assessment of Pre-Seismic Code Buildings and Emergency Facilities in the UAE. In: Second European Conference on Earthquake Engineering and Seismology. Istanbul

Jaiswal K, Wald D, Porter K (2010) A global building inventory for earthquake loss estimation and risk management. Earthq Spectra 26:731–748. https://doi.org/10.1193/1.3450316

Jalayer F, De Risi R, Manfredi G (2015) Bayesian Cloud Analysis: Efficient structural fragility assessment using linear regression. Bull Earthq Eng 13:1183–1203. https://doi.org/10.1007/s10518-014-9692-z

Jaradat R, Fahjan Y, Nuseir O, Awawdeh M, Al-Qaryouti M, Diabat A, Abdulla A-R (2008) Earthquake risk assessment of Greater Amman Municipality. UNDP project. https://www.researchgate.net/publication/267927125_Earthquake_risk_assessment_of_Greater_Amman_Municipality_UNDP_project_2008_under_Atlas_no_51485_Jaradat_R_A_Awawdeh_M_M_Fahjan_Y_Al-Qaryouti_M_Y_Nusier_O_K_Diabat_A_A_and_Al-Rawabdeh_A_M. Accessed 24 Apr 2019

Jiménez MJ, Giardini D, Grünthal G (2003) The ESC-SESAME Unified Hazard Model for the European-Mediterranean region. CSEM / EMSC Newsl. 19:2–4

Jiménez MJ, Giardini D, Grünthal G, Erdik M, García-Fernández M, Lapajne J, Makropoulos K, Musson R, et al (2001) Unified seismic hazard modelling throughout the Mediterranean region. Boll di Geofis Teor ed Appl 42:3–18

Kelman I, Spence R (2004) An overview of flood actions on buildings. Eng Geol 73:297–309. https://doi.org/10.1016/J.ENGGEO.2004.01.010

Mahmoud SH, Gan TY (2018) Multi-criteria approach to develop flood susceptibility maps in arid regions of Middle East. J Clean Prod 196:216–229. https://doi.org/10.1016/j.jclepro.2018.06.047

Makhoul N, Navarro C, Lee J, Abi-youness A (2016) Assessment of seismic damage to buildings in resilient Byblos City. Int J Disaster Risk Reduct 18:12–22. https://doi.org/10.1016/j.ijdrr.2016.05.007

Maqsood T, Wehner M, Ryu H, Edwards M, Dale K, Miller V (2014) GAR15 Regional Vulnerability Functions: Reporting on the UNISDR/GA SE Asian Regional Workshop on Structural Vulnerability Models for the GAR Global Risk Assessment, 11-14 November, 2013, Geoscience Australia, Canberra, Australia. http://dx.doi.org/10.1163

Martins L, Silva V (2020) Development of a Fragility and Vulnerability Model for Global Seismic Risk Analyses. Bull Earthq Eng. https://github.com/lmartins88/global_fragility_vulnerability, in review

Merz B, Kreibich H, Schwarze R, Thieken A (2010) Review article "Assessment of economic flood damage" Nat Hazards Earth Syst Sci 10:1697–1724. https://doi.org/10.5194/nhess-10-1697-2010

Messner F, Penning-rowsell E, Green C, Tunstall S, Veen A Van Der (2007) Evaluating flood damages: guidance and recommendations on principles and methods

Mohindra R, Nair AKS, Gupta S, Sur U, Sokolov V (2012) Probabilistic seismic hazard analysis for Yemen. Int J Geophys 2012:. https://doi.org/10.1155/2012/304235

Motamed H, Calderon A, Silva V, Costa C (2019) Development of a probabilistic earthquake loss model for Iran. Bull Earthq Eng 17:1795–1823. https://doi.org/10.1007/s10518-018-0515-5

Neal J, Schumann G, Bates P (2012) A subgrid channel model for simulating river hydraulics and floodplain inundation over large and data sparse areas. Water Resour Res 48:. https://doi.org/10.1029/2012WR012514

OCHA (2015) Humanitarian Bulletin: Iraq. https://reliefweb.int/sites/reliefweb.int/files/resources/OCHA Iraq Humanitarian Bulletin 16 October - 5 November 2015 %28issued 151108%29-.pdf. Accessed 12 Nov 2019

Olsen A, Zhou Q, Linde J, Arnbjerg-Nielsen K (2015) Comparing Methods of Calculating Expected Annual Damage in Urban Pluvial Flood Risk Assessments. Water 7:255–270. https://doi.org/10.3390/w7010255

Ordaz MG, Cardona OD, Salgado-Gálvez MA, Bernal-Granados GA, Singh SK, Zuloaga-Romero D (2014) Probabilistic seismic hazard assessment at global level. Int J Disaster Risk Reduct 10:419–427. https://doi.org/10.1016/j.ijdrr.2014.05.004

Pagani M, García-Pelaez J, Gee R, Johnson KL, Silva V, Simionato M, Styron R (2020) The global earthquake model

(GEM) seismic hazard map. Earthq Spectra, in press.

Pagani M, Monelli D, Weatherill G, Danciu L, Crowley H, Silva V, Henshaw P, Butler L, et al (2014) OpenQuake Engine: An Open Hazard (and Risk) Software for the Global Earthquake Model. Seismol Res Lett 85:692–702

Pascucci V, Free MW, Lubkowski ZA (2008) Seismic Hazard And Seismic Design Requirements for The Arabian Peninsula Region. In: The 14 World Conference on Earthquake Engineering (14 WCEE). Beijing, China

Petrovski J. (1983) Engineering measures for earthquake risk reduction in the Arab countries, in Assessment and Mitigation of Earthquake Risk in the Arab Region (Cidlinsky K., and B. M. Rouhban, eds.), Prepared by UNESCO for the Arab Fund for Economic and Social Development. https://unesdoc.unesco.org/ark:/48223/pf0000080106. Accessed 24 Apr 2019

Rudari R, Silvestro F, Campo L, Rebora N, Boni G, Herold C (2015) Improvement of The Global Flood Model For The GAR 2015. UNISDR

Sampson CC, Smith AM, Bates PD, Neal JC, Alfieri L, Freer JE (2015) A high-resolution global flood hazard model. Water Resour Res 51:7358–7381. https://doi.org/10.1002/2015WR016954

ŞEN Z (2008) Wadi Hydrology. CRC PRESS, New York

Silva V, Amo-Oduro D, Calderon A, Costa C, Dabbeek J, Despotaki V, Martins L, Pagani M, et al (2020) Development of a global seismic risk model. Earthq Spectra 875529301989995. https://doi.org/10.1177/8755293019899953

Silva V, Crowley H, Pagani M, Monelli D, Pinho R (2014) Development of the OpenQuake engine, the Global Earthquake Model's open-source software for seismic risk assessment. Nat Hazards 72:1409–1427. https://doi.org/10.1007/s11069-013-0618-x

Silva V, Yepes-Estrada C, Dabbeek J, Martins L, Brzev S (2018) GED4ALL - Global Exposure Database for Multi-Hazard Risk Analysis – Multi-Hazard Exposure Taxonomy. GEM Technical Report 2018-01. GEM Foundation, Pavia, Italy

Smith A, Sampson C, Bates P (2015) Regional flood frequency analysis at the global scale. Water Resour Res 51:539–553. https://doi.org/10.1002/2014WR015814

Sokolov V, Zahran HM, Youssef SE-H, El-Hadidy M, Alraddadi WW (2017) Probabilistic seismic hazard assessment for Saudi Arabia using spatially smoothed seismicity and analysis of hazard uncertainty. Bull Earthq Eng 15:2695–2735. https://doi.org/10.1007/s10518-016-0075-5

UBC (1997) Uniform Building Code, International Conference of Building Officials, Whittier, California.

UNDRR (2019) Global Assesment Report on Disaster Risk Reduction. Geneva, Switzerland

UNISDR, EM-DAT (2018) Economic Losses, Poverty and Disasters 1998-2017.

Ward PJ, de Moel H, Aerts JCJH (2011) How are flood risk estimates affected by the choice of return-periods? Nat Hazards Earth Syst Sci 11:3181–3195. https://doi.org/10.5194/nhess-11-3181-2011

Yaseen AA, Begg D, Nanos N (2015) Seismic fragility assessment of low-rise unreinforced masonry buildings in the Kurdistan region of Iraq. Int J Struct Anal Des 2:1–9

Yepes-Estrada C, Silva V, Rossetto T, D'Ayala D, Ioannou I, Meslem A, Crowley H (2016) The global earthquake model physical vulnerability database. Earthq Spectra 32:2567–2585. https://doi.org/10.1193/011816EQS015DP

Zahran HM, Sokolov V, Youssef SEH, Alraddadi WW (2015) Preliminary probabilistic seismic hazard assessment for the Kingdom of Saudi Arabia based on combined areal source model: Monte Carlo approach and sensitivity analyses. Soil Dyn Earthq Eng 77:453–468. https://doi.org/10.1016/j.soildyn.2015.06.011

Zare M, Amini H, Yazdi P, Sesetyan K, Demircioglu MB, Kalafat D, Erdik M, Giardini D, et al (2014) Recent developments of the Middle East catalog. J Seismol 18:749–772. https://doi.org/10.1007/s10950-014-9444-1